A New Current Mode Fuzzy Logic Controller with Extended State Observer for DC-to-DC Converters

Guang Feng, Wanfeng Zhang, Yan-Fei Liu
Department of Electrical and Computer Engineering, Queen's University,
Kingston, Ontario, Canada, K7L 3N6
guang.feng@ece.queensu.ca, wanfeng.zhang@ece.queensu.ca, yanfei.liu@ece.queensu.ca

Abstract — **This paper introduces a new fuzzy logic controller (FLC) using inductor current feedback to improve the dynamic performance of DC-to-DC converters. Based on the feedback of the inductor current, the new control method combines the merits of both the conventional FLC and current mode control. Therefore, the dynamic performance of power converter system is significantly improved. Furthermore, in order to eliminate the influence of load variation, extended state observer (ESO) is developed. By using ESO, the influence of load disturbances is accurately estimated and compensated. Experimental results demonstrated that the proposed methods ensure good robustness under supply voltage changes, load current variation, and reference voltage changes. Substantial improvement of dynamic performances such as small overshoot, more damping and fast transient response is also achieved.**

Keywords - fuzzy logic controller; current feedback; extended state observer; robustness

I. INTRODUCTION

With the rapid development of advanced high-speed digital control circuits, intelligent power supplies are expected to play an important role in communication, computer and aerospace industries in the near future. Among many available digital control methods, fuzzy logic controller (FLC) has emerged as one of the most promising control methods in the power electronics due to its capability of fast computation with high precision. FLC has been proven to be superior to the conventional PID controller in that it naturally provides the ability to deal with highly nonlinear and time-variant systems where the mathematical models are difficult to be obtained [1]. Thus, it is well suited in resolving the time-varying nonlinear nature of switches in DC-to-DC converters [2,3]. Conventional FLC, which utilizes the output voltage error and the change of error as its input, has been widely used in the past few years, but its dynamic performance is not satisfactory.

In order to improve the dynamic performance of power converters, a new current mode fuzzy logic control method is proposed and demonstrated in this paper. This new control law is based on the introduction of inductor current feedback into the inner control loop of converter system, where FLC serves as the outer control loop. The proposed topology combines the merits of both the conventional FLC and current mode control. Therefore, instantaneous correction action against input voltage changes is achieved. This methodology can be easily applied to many converter topologies such as Buck, Boost and Buck-Boost converters.

In addition, in order to further improve the dynamic performance under load change, a new configuration called extended state observer (ESO) is developed. By using ESO, accurate estimation and compensation of load change are achieved. The proposed fuzzy logic controller with ESO has the advantage of good robustness, which leads to very good steady state and dynamic performance even in presence of strong and fast variation of input voltage change, load current change and reference voltage change.

Experiments are performed in Boost converter to verify the effectiveness of the proposed fuzzy logic controller with ESO. Results confirmed that the proposed methods achieve much better robustness in terms of input voltage change, load change and reference voltage change. Better dynamic performance, such as small overshoot, more damping and fast transient time, has been achieved.

II. BASIC OPERATION PRINCIPLE OF THE PROPOSED FUZZY LOGIC CONTROLLER USING INDUCTOR CURRENT FEEDBACK

The inductor current plays a very important role in high performance DC-to-DC converter control. It can provide additional information on the energy stored in the converter [4]. Given Boost converter as an example, Fig. 1 shows the average equivalent circuit model of Boost converter. It can be seen from the model that the output voltage is fed by a current, which can be represented as $i_L - d \cdot i_L = (1-d)i_L$. If i_L is directly controlled, then $(1-d)i_L$ can be considered approximately as a current source [5]. Therefore, the whole circuit behaves as if the output capacitor C and load resistor R_o were fed by a current source $(1-d)i_L$. In small signal control-to-output transfer function, the pole of the system is mainly associated with R_o and C as if the inductor L were not there. It contains one less pole than the conventional FLC without current feedback. This configuration simplifies the mathematical model and makes the system easier to control and consequently, the dynamic performance will be improved.

In this paper, the proposed fuzzy logic control using inductor current feedback is implemented with two control loops (shown in Fig. 2). The outer loop is the voltage loop, and

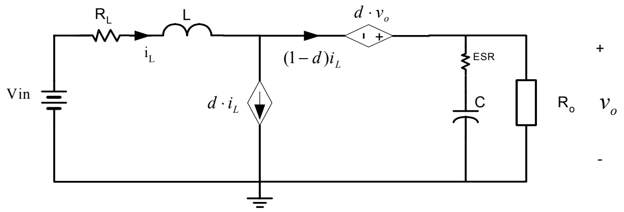

Figure 1. Average circuit model of Boost converter

the inner loop is the current loop. The output of the voltage loop serves as the reference of the inductor current.

As shown in Fig. 2, Boost converter is used as an example, its average value model can be described as:

$$\frac{di_L}{dt} = -\frac{R_L}{L} \cdot i_L - \frac{1-d}{L} \cdot v_o + \frac{1}{L} v_{in} \quad (1)$$

$$\frac{dv_o}{dt} = \frac{1-d}{C} \cdot i_L - \frac{1}{C} \cdot \frac{v_o}{R_o} \quad (2)$$

where i_L , v_o, v_{in} are the inductor current, output DC voltage and supply DC voltage, d is the duty cycle, R_o is the load resistor and R_L is the winding resistor of the inductor.

Equation (2) can be rewritten as $i_L = \frac{C}{1-d}\frac{dv_o}{dt} + \frac{1}{1-d} \cdot \frac{v_o}{R_o}$. It can be observed that the inductor current contains the information about the derivatives of the output voltage. By using the inductor current into FLC, the dynamic response of whole system could be significantly improved. This approach will allow substantial improvement of converter dynamic performances similarly to that obtained in analog current mode controlled converters.

The voltage control loop can be implemented by a Proportional-Differential (PD) like FLC combined with a digital integrator (as shown in Fig. 2). The inputs of PD like FLC are defined as the error of output voltage $e_u(k)$ and the change of error $ce_u(k)$. Seven fuzzy levels are defined for e_u and ce_u. The input membership functions chosen for e_u and ce_u are triangular ones with 50% overlap. The membership functions of output variable i_{Lref_P} are 7-level triangular fuzzy-set values. The min-max method of inference engine is used. The defuzzify method used in this FLC is the Center of Area. The fuzzy control rules for voltage loop are shown in Table I.

The output of the fuzzy logic controller i_{Lref_P} is the proportional part of reference current i_{Lref}. Combined with the output of integrator i_{Lref_I}, it constitutes the reference current signal i_{Lref} , which can be represented as $i_{Lref} = i_{Lref\_P} + i_{Lref\_I}$. Based on this algorithm, there is no steady error and fast large-signal dynamic response with small overshoot can be achieved with proper selection of proportional and integral efficients.

In the inner control loop, the difference between the sensed inductor current i_L and the reference current signal i_{Lref} can be processed by PID controller or another fuzzy logic controller which will generate the duty cycle $d(k)$. Different from analog current mode control, the duty cycle d is directly calculated, so the comparator and artificial ramp are not needed any more. Therefore, the problems of susceptibility to noise and sub-harmonic oscillation for duty cycle greater than 0.5, which exist in analog peak current control method, are eliminated inherently, as observed in the experimental results.

The proposed FLC method that uses inductor current feedback has significant advantages. First, the inductor current is directly controlled by the inner control loop. Therefore, it has essentially no phase lag from control to inductor current and the pole related to the inductor is eliminated. This helps to achieve feedback loop stabilization. Second, because the change in the inductor current is sensed earlier than the change in the output voltage, the proposed control algorithm achieves instantaneous correction action against line voltage changes without having to wait for a sensed output voltage change to pass through the relatively long delay in a conventional FLC (without current feedback). Therefore, the reaction of control system will begin earlier and be faster than the case when only the output voltage is sensed. Third, it has inherent current limiting, making the power converter nearly immune to damage from overloads. Fourth, with the information contained in the feedback inductor current, the advanced control algorithm could be used to improve the dynamic performance on load current regulation.

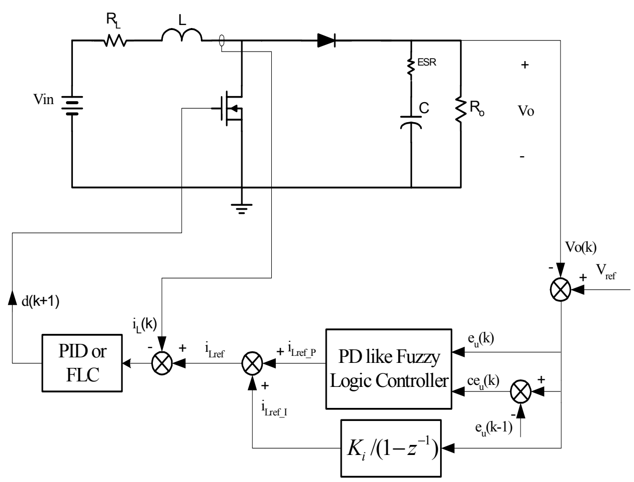

Figure 2. Block diagram of current mode fuzzy logic controller using i_L in the inner control loop

TABLE I. THE RULE BASE OF FLC IN TABULAR FORM

ce\e	NB	NM	NS	ZE	PS	PM	PB
NB	NB	NB	NB	NB	NM	NS	ZE
NM	NB	NB	NB	NM	NS	ZE	PS
NS	NB	NB	NM	NS	ZE	PS	PM
ZE	NB	NM	NS	ZE	PS	PM	PB
PS	NM	NS	ZE	PS	PM	PB	PB
PM	NS	ZE	PS	PM	PB	PB	PB
PB	ZE	PS	PM	PB	PB	PB	PB

III. INTRODUCTION OF EXTENDED STATE OBSERVER

In section II, inductor current feedback is utilized to improve the dynamic performance of Boost converter under line voltage changes. In order to improve the dynamic performance of load change even further, extended state observer is used in the proposed control system. By using nonlinear state feedback, extended state observer can achieve instantaneous estimation and compensation of the load current change. As a consequence, the overshoot and response time of the system under load change are decreased significantly.

A.. Advantages of Nonlinear Feedback Compared with Linear Feedback

In many respects, nonlinear feedback has some high efficient characteristics compared to linear feedback. To give a simple example, for the 1st order state observer $\dot{x} = -cx + u$, where its input signal is $v(t)$ and c is a constant related to the system. Feedback control $u(t) = f(v(t) - x(t))$ is designed to make the state variable $x(t)$ converge to the input signal $v(t)$ quickly. For simplification, we assume input $v(t) = v$ (constant). The linear feedback is chosen as: $u = k(v(t) - x(t))$, where k is the feedback coefficient. Then, the steady state error of the observer $e_{linear}(t) = v(t) - x(t)$ is converged to $v \cdot c/(c+k)$. Appendix gives the detailed derivation.

However, if a nonlinear feedback is chosen as $u = k|v(t) - x|^{a}\, sign(v(t) - x)$ ($0 < \alpha < 1$), the steady state error $e_{nonlinear}(t)$ will be smaller than $(\frac{cv}{k})^{\frac{1}{\alpha}}$, as shown in Appendix. Appendix also illustrates that in the condition of $0 < \alpha < 1$, $c << k$ and $cv << k$, which is normally the case, the steady state error of nonlinear feedback $e_{nonlinear}$ will be much smaller than that of linear feedback using the same feedback coefficient k. For example, if $c = 1$, $v = 1$ and $k = 100$, the steady state error by using linear feedback is $e_{linear} = \frac{1}{101} \approx \frac{1}{100}$. By using nonlinear feedback, and assume $\alpha = \frac{1}{2}$, the steady state error $e_{nonlinear} < (\frac{1}{100})^2 << e_{linear}$.

From the above example, it can be observed that the nonlinear feedback has the ability to greatly improve the accuracy and efficiency of system state observation.

B. Principle of Extended State Observer

ESO is a nonlinear configuration, which uses nonlinear state feedback to achieve the states and disturbances observation of the system without knowing its exact parameters. Giving an example, for any arbitrary N^{th} order nonlinear system

$$x^{(n)} = f(x, \dot{x}, \cdots, x^{(n-1)}, t) + w(t) + c \cdot u(t) \quad (3)$$

where $f(t)$ represents the arbitrary system function, $w(t)$ is an unknown disturbance, $u(t)$ is the control law, $x(t)$ is the measurable state variable, and c is the coefficient of control law.

Its state space equation can be written as:

$$\begin{cases} \dot{x}_1 = x_2 \\ \vdots \\ \dot{x}_{n-1} = x_n \\ \dot{x}_n = f(x, \dot{x}, \cdots, x^{(n-1)}, t) + w(t) + cu \end{cases} \quad (4)$$

where $x_1 = x,\ x_2 = \dot{x}, \cdots, x_n = x^{(n-1)}$.

From (4), we can observe that there are N state variables $x_1,\ x_2, \cdots, x_n$ in the N^{th} order nonlinear system. In addition, internal and external disturbance $w(t)$ is unknown in the real time implementation. By appending $w(t)$ as another state variable, there are $N+1$ state variables existing in the nonlinear system, which are needed to be sensed or observed. For the time-varying system, the state space variables can be obtained successfully by designing a state observer. Unlike the full order (N^{th} order) state observer, ESO utilizes $(N+1)^{th}$ order (full order plus 1) state observation to achieve state and disturbance estimation (shown in (5)). After start up, the output of the ESO $z_1, \cdots, z_n$ will converge quickly and accurately to the observed states $x_1,\ x_2, \cdots, x_n$. The output of ESO z_{n+1} will achieve the estimation of disturbance $w(t)$. The initial values of $z_1, \cdots, z_n, z_{n+1}$ are all set to 0. Equation (5) shows the mathematical modeling of $(N+1)^{th}$ extended state observer.

$$\begin{cases} \dot{z}_1 = z_2 - g_1(z_1 - x_1(t)) \\ \vdots \\ \vdots \\ \dot{z}_n = z_{n+1} - g_n(z_1 - x_1(t)) + c \cdot u(t) \\ \dot{z}_{n+1} = -g_{n+1}(z_1 - x_1(t)) \end{cases} \quad (5)$$

$$g_i(z_1 - x_1(t)) = \beta_i \cdot fal(z_1 - x_1(t), \alpha_i, \delta) \qquad i = 1, \cdots, n+1$$

$$fal(\varepsilon, \alpha_i, \delta) = \begin{cases} |\varepsilon|^{\alpha_i}\ \mathrm{sgn}(\varepsilon), & |\varepsilon| > \delta \\ \varepsilon / \delta^{1-\alpha_i}, & |\varepsilon| \le \delta \end{cases}$$

where $\varepsilon = z_1 - x_1(t)$, $\mathrm{sgn}(\varepsilon)$ is the signum function, and $\alpha_i, \beta_i, \delta$ are the parameters of ESO.

It can be observed from (5) that the structure of ESO is mainly based on the switching functions $fal(z_1 - x_1, \alpha_i, \delta)$. The mathematical model of $fal(z_1 - x_1, \alpha_i, \delta)$ is a nonlinear structure with linear intervals near the original point (shown in Fig. 3). The merit of this topology is that it can fully utilize the nonlinear feedback characteristics for large signals. At the same time, the phenomenon of chatting near the origin is avoided. In the linear intervals, extended state observer acts as a low pass filter.

If we define $x_{n+1}(t) = f(x, \dot{x}, \cdots, x^{(n-1)}, t) + w(t)$, then (4) can be rewritten as:

$$\begin{cases} \dot{x}_1(t) = x_2(t) \\ \quad\vdots \\ \dot{x}_n(t) = x_{n+1}(t) + c \cdot u(t) \\ \dot{x}_{n+1}(t) = b(t) \end{cases} \tag{6}$$

where $b(t)$ is the variation rate of system function and disturbance $x_{n+1}(t)$. In real case, the value of $b(t)$ is unknown, and we need not to know it. The only thing we care is that the value of $b(t)$ should be finite during the transient, which is always true in the real time implementation.

Subtracting (6) from (5), the dynamic error equation is derived as

$$\begin{cases} \Delta\dot{x}_1 = \Delta x_2 - g_1(\Delta x_1) \\ \quad\vdots \\ \Delta\dot{x}_n = \Delta x_{n+1} - g_n(\Delta x_1) \\ \Delta\dot{x}_{n+1} = -b(t) - g_{n+1}(\Delta x_1) \end{cases} \tag{7}$$

where $\Delta x_i = z_i - x_i, \quad i = 1, \cdots, n+1$

In real case, $b(t)$ is finite. Then, when the nonlinear functions $g_i(z)$ and their related parameters $\alpha_i, \beta_i, \delta$ are properly selected, the system (7) is asymptotic stable [6]. Under this condition, the state variables of ESO, $z_i(t)$, $i = 1, \cdots, n$, will quickly converge to the observed state variables $x(t)$ and its derivatives $\dot{x}(t), \ddot{x}(t), \cdots, x^{(n-1)}(t)$. Furthermore, the overall effect of the external and internal disturbances $x_{n+1}(t)$ imposed on the system can be observed by $(N+1)^{th}$ state variable $z_{n+1}(t)$ successfully, even though the mathematic expression and accurate parameters of $f(t)$ and $w(t)$ may be still unknown. Based on this information, instantaneous compensation of disturbances can be achieved. It will greatly enhance the robustness of the control system against the modeling uncertainties and disturbances.

C. Extended State Observer Applied to Boost Converter Control System

In Boost converter, ESO is used in the voltage control loop to improve the dynamic performance and robustness under load current disturbance Δi_o (shown in Fig. 4). The inputs of ESO are the sensed inductor current, output voltage and the duty cycle calculated in the previous sampling period. The output of ESO is the dynamic compensation of the disturbance $\Delta i_L(k)$.

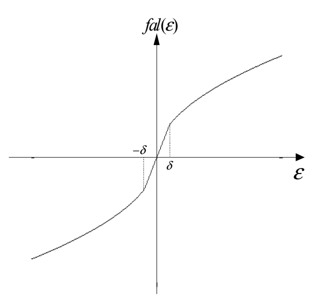

Figure 3. The figure of switching function $fal(\varepsilon)$

The state equation (2) of Boost converter can be rewritten as follows [7]:

$$\frac{dv_o}{dt} = \frac{1-d}{C} \cdot i_L - \frac{1}{C} \cdot \left(\frac{v_o}{R_o} + \Delta i_o\right) = \frac{1-d}{C} \cdot i_L - \frac{1}{C} \cdot \frac{v_o}{R_o} + w_1(t) \tag{8}$$

where $w_1(t) = -\frac{1}{C}\Delta i_o$.

Based on (8), the external load change is treated as disturbances imposed on the Boost converter system. To estimate and compensate for the system disturbance, a 2nd order ESO for the voltage control loop is used,

$$\begin{cases} \dot{z}_1 = z_2 - g_1(z_1 - v_o) - \frac{1}{C} \cdot \frac{v_o}{R_o} + \frac{1-d}{C} i_L \\ \dot{z}_2 = -g_2(z_1 - v_o) \end{cases} \tag{9}$$

$$\Delta i_L(t) = -z_2(t)/(1-d) * C$$

where $g_i(\varepsilon) = \begin{cases} \beta_i \cdot |\varepsilon|^{\frac{1}{2}} \cdot \mathrm{sgn}(\varepsilon) & |\varepsilon| > \delta \\ \beta_i \cdot \varepsilon / \delta^{\frac{1}{2}} & |\varepsilon| \le \delta \end{cases} \quad i = 1,2$,

$\varepsilon = z_1 - v_o$, and β_i, δ are the variable parameters of ESO.

When the nonlinear functions $g_i(z)$ and their related parameters are properly selected, the external disturbance $w_1(t)$ imposed on the Boost converter system can be observed by the 2nd state of ESO $z_2(t)$. Based on this information, on line compensation of load disturbances can be made by $\Delta i_L(t) = -z_2(t)/(1-d) * C$. It will greatly enhance the robustness of the control system against load disturbances. In addition, all these functions and parameters of ESO do not depend on the accurate mathematical model of power converters. Therefore, this observer has good robustness and adaptability. This is the main advantage of this configuration. It can be seen from (9) that, the calculation of ESO is composed of a division, a square root and several addition and multiplication. Therefore, it is easy to be realized in hardware implementation.

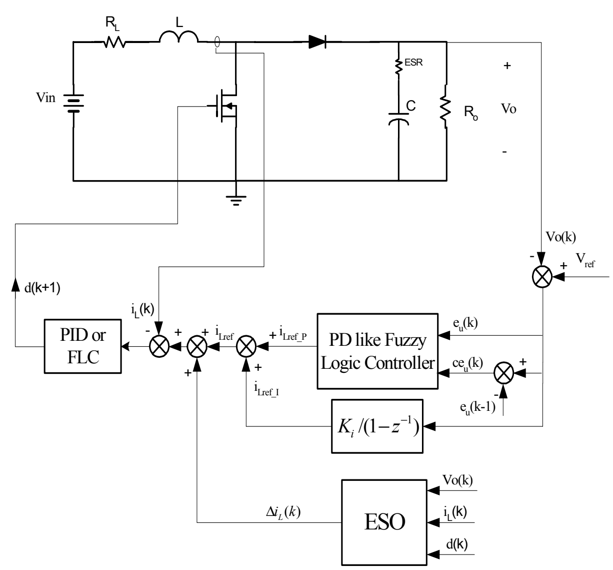

Figure 4. Block diagram of current mode fuzzy logic controller with ESO

IV. EXPERIMENTAL RESULTS

A Boost converter control system with the proposed current mode FLC and ESO was built to verify the above analysis. An FPGA (200K gates) was used as the core of the fuzzy logic controller and extended state observer. The design is shown in Fig. 5. The output voltage and inductor current are sensed and feedback to FPGA by two 8-bit A/D converters. The PWM signal is calculated and generated by the control algorithms inside FPGA. The parameters of Boost converter are listed as following: input voltage $V_{in} = 15V$, output voltage $V_o = 30V$, $L = 24uH$, $C = 220uF$, ESR = 0.06Ω, R_L=0.04Ω, where ESR is the equivalent series resistor of the output capacitor and R_L is the winding resistor of the inductor.

The dynamic performance of the conventional FLC and the proposed FLC using current feedback with ESO are compared under the same operating condition. All of the controller parameters are optimized at the operating condition $V_{in} = 15V$, $V_o = 30V$, I_{load}=1.5 A, $L = 24uH$, $C = 220uF$ to make the system have lowest overshoot and fastest response time under input voltage change and load variation. All these parameters are then kept unchanged during the experiments.

Considering the dynamic performance, the proposed algorithm is verified under large variation of input voltage (from 15V to 19V), and load current (from 1A to 3A) in Boost converters (as shown in Fig. 6-7).

It is shown from Fig. 6 that by using the proposed FLC with ESO, the overshoot due to input voltage change is decreased to almost 40% compared with the conventional FLC. The damping is also significantly improved and the recovery time is greatly reduced.

When the load current changes, by using the proposed current mode FLC with ESO, the overshoot is decreased to 60% of that of the conventional FLC. The damping is improved and the recovery time is reduced, too (shown in Fig. 7).

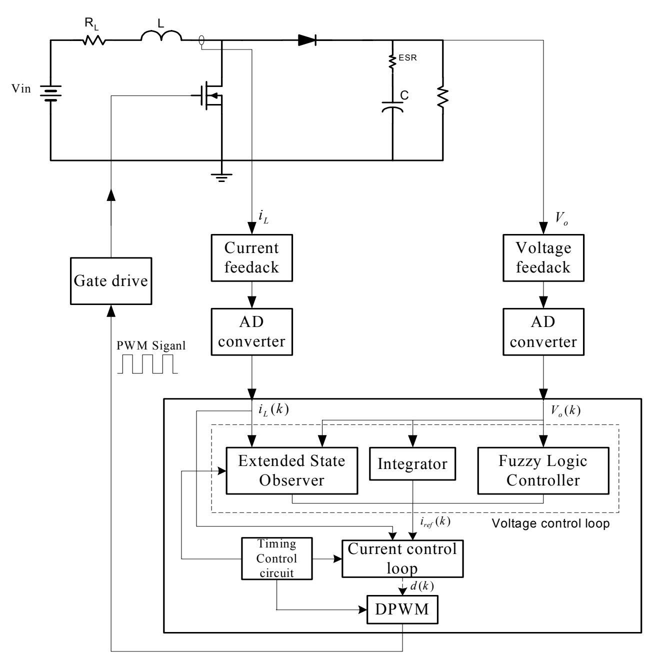

Figure 5. Diagram of experimental test bench using FPGA

In order to evaluate the dynamic performance of the system under wide operating range, the conventional FLC and proposed FLC with ESO are applied to regulate Boost converter under different input voltage without changing controller parameters (shown in Fig. 8-10). First, experiments on output reference voltage changes (from 30V to 36V) at rated input voltage (Vin=15V) and load resistor R_o=20Ω are performed (shown in Fig. 8). It is shown that the overshoot achieved in the proposed FLC system is much smaller than that of conventional FLC. Furthermore, its recovery time is less than that of the conventional FLC algorithm.

Fig. 9-10 show the experimental results of the output voltage change at different input voltages. It is shown that the overshoot of the system using conventional FLC changes significantly under different input voltages. But the proposed algorithm can still maintain good dynamic performance such as small overshoot in spite of input voltage changes.

V. CONCLUSION

In this paper, a new current mode fuzzy logic controller with extended state observer for DC-to-DC converters is proposed and demonstrated. With the feedback of inductor current, the proposed scheme combines the advantages of both the conventional FLC and current mode control. By using ESO, the load change is accurately estimated and compensated. The dynamic performance of power converter system is significantly improved. Comparisons are made in details between the proposed methods and the conventional FLC. Experimental results show that the proposed control methods produce much better dynamic performance and robustness than the conventional FLC in terms of input voltage change, load current variation and reference voltage change. All these benefits open new perspectives on utilization of intelligent control on DC-to-DC converters, and indicate that such schemes can be an attractive alternative to the classic controller in power converter applications where high dynamic performance is preferred.

REFERENCE

[1] D. Driankov, H. Hellendoorn and M. Reinfrank, An Introduction to Fuzzy Control, 2nd edition, Springer, 1996.

[2] C. K. Lau and M. H. Pong, “DSP based fuzzy controlled power converter operating in both continuous and discontinuous conduction modes,” IEEE IECON’96, vol. 3, 1996, pp. 1530 –1535.

[3] F. H. Wang and C. Q. Lee, “Comparison of fuzzy logic and current-mode control techniques in buck, boost and buck/boost converters,” IEEE PESC’95, vol. 2, 1995, pp. 1079 –1085.

[4] B. Tomescu and H. F. Vanlandingham, “Improved large-signal performance of paralleled DC-DC converters current sharing using fuzzy logic control,” IEEE Transactions on Power Electronics, vol. 14, no. 3, 1999, pp. 573-577.

[5] Yan-Fei Liu and P.C. Sen, “A general unified large signal model for current programmed DC-to-DC converters”, IEEE Transactions on Power Electronics, vol. 9, no. 4, 1994, pp. 414 – 424.

[6] J. Han, "Auto-disturbances-rejection Controller and It's Applications", Trans. Control and Decision, China, vol.13, no.1, pp19-23, 1998.

[7] Guang Feng, W. Zhang, Y. F. Liu, "An Adaptive Current Mode Fuzzy Logic Controller for DC-to-DC Converters", IEEE APEC 2003, vol. 2 , pp. 983 -989.

APEENDIX. STEADY STATE ERROR ANALYSIS

This appendix analyzes the steady state error for linear feedback and nonlinear feedback applied to state observer. In the example of the section III, a 1st order state observer $\dot{x} = -cx + u$ is used. Without losing generality, we assume that $c > 0$ and the reference value of x is v, where v is constant and $v > 0$.

By using the linear feedback $u = k(v - x(t))$, where $k > 0$, in the steady state, $\dot{x} = 0$. Then, we can get $x = \frac{k}{c+k} v$.

Therefore, the steady state error under linear feedback $u = k(v - x(t))$ is

$$e_{linear} = v - x = \frac{c}{c+k} v \tag{A–1}$$

From (A-1), we can see that

$$e_{linear} \approx \frac{c}{k} v, \quad if \quad c << k \tag{A–2}$$

For the nonlinear feedback $u = k|v - x(t)|^{\alpha} sign(v - x(t))$, $0 < \alpha < 1$, k is chosen to be the same value as that used in the linear feedback.

Without losing generality, we can assume that in the steady state, $0 < x < v$ and the steady state error under nonlinear feedback is $e_{nonlinear} = v - x > 0$. Otherwise, if in the steady state, $0<v<x$, from the function $\dot{x} = -cx + u$ and $u = k|v - x|^{\alpha} sign(v - x)$, we can get that at this condition $\dot{x} < 0$. The observer will be in the dynamic transients again.

In the steady state, $\dot{x} = 0$. Then,

$$k(v - x)^{\alpha} = cx \tag{A–3}$$

Dividing both sides of (A-3) by v^{α}, the following equation can be derived:

$$k(1 - \frac{x}{v})^{\alpha} = \frac{cx}{v^{\alpha}} \tag{A–4}$$

When considering $0 < x < v$, (A-4) can be rewritten as

$$k(1 - \frac{x}{v})^{\alpha} = \frac{cx}{v^{\alpha}} = c \cdot (\frac{x}{v}) \cdot v^{1-\alpha} < cv^{1-\alpha} \tag{A–5}$$

Rearrange (A-5), the following relation can be derived

$$(1 - \frac{x}{v}) < (\frac{c}{k})^{\frac{1}{\alpha}} v^{\frac{1-\alpha}{\alpha}} \tag{A–6}$$

Multiply both sides of (A-6) by v, the relation of steady state error under nonlinear control can be derived as:

$$e_{nonlinear} = v - x < (\frac{c}{k})^{\frac{1}{\alpha}} \cdot v^{\frac{1}{\alpha}} \tag{A–7}$$

Comparing (A-2) and (A-7), it can be observed that if $c << k$, $cv << k$ and $0 < \alpha < 1$,

$$\frac{e_{nonlinear}}{e_{linear}} < (\frac{cv}{k})^{\frac{1}{\alpha} - 1} \tag{A–8}$$

For example, if $c = 1$, $v = 1$, $k = 100$, and $\alpha = \frac{1}{2}$, then $e_{linear} \approx 0.01$, $e_{nonlinear} < 0.01^2 = 0.0001$ and $\frac{e_{nonlinear}}{e_{linear}} < 0.01$.

From the above analysis, it verifies that by using nonlinear feedback, the steady error of the observer is much less than that using linear feedback if k is selected large enough.

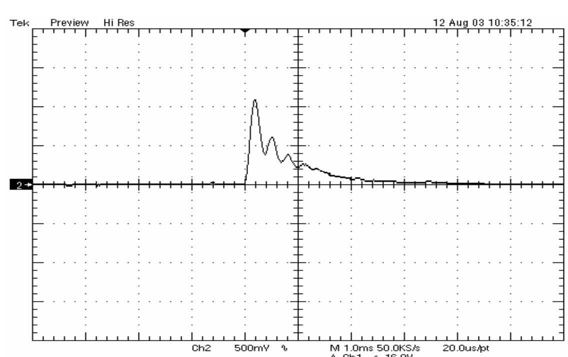

(a) Conventional fuzzy logic controller

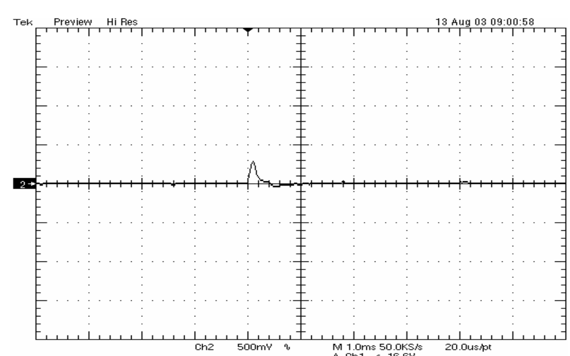

(b) Current mode fuzzy logic controller with ESO

Figure 6. Output voltage response to input voltage change from 15to 19V (X axis: 1ms/div; Y axis: 500mV/div)

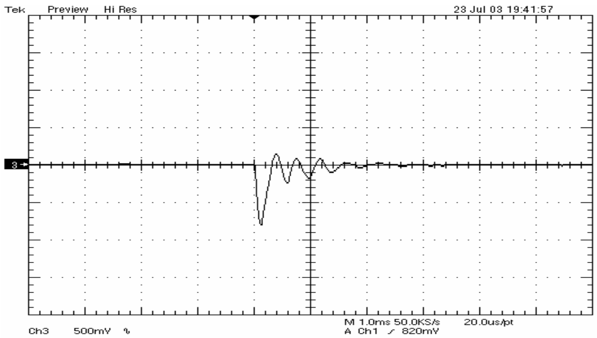

(a) Conventional fuzzy logic controller

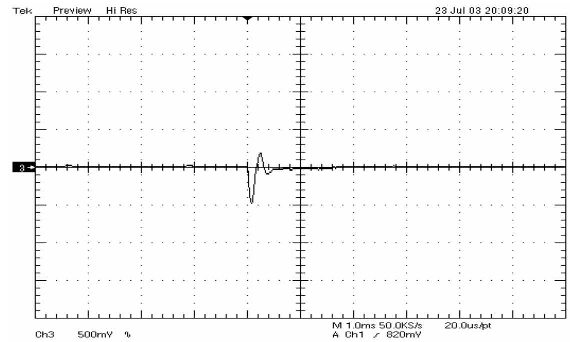

(b) Current mode fuzzy logic controller with ESO

Figure 7. Output voltage response to load current change from 1A to 3A (X axis: 1ms/div; Y axis: 500mV/div)

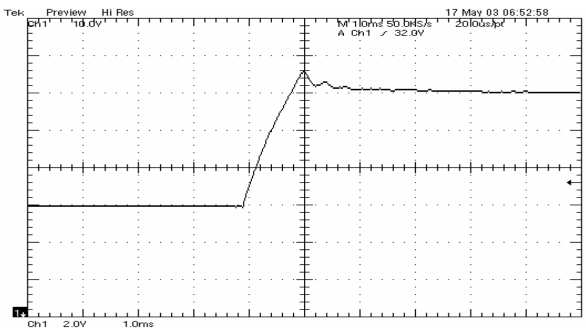

(a) Conventional fuzzy logic controller

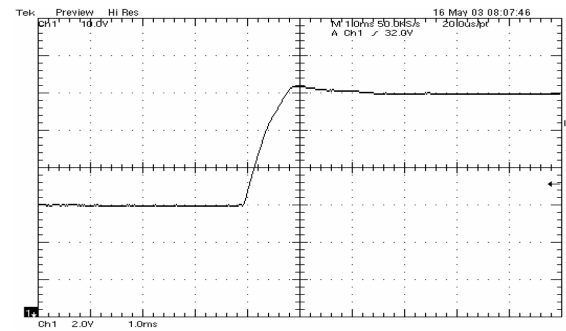

(b) Current mode fuzzy logic controller with ESO

Figure 8. Step change (from 30 to 36V) in output reference voltage for Vin=15V (X axis: 1ms/div, Y axis: 2V/div)

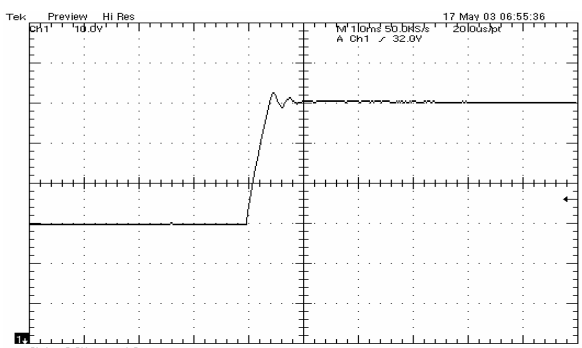

(a) Conventional fuzzy logic controller

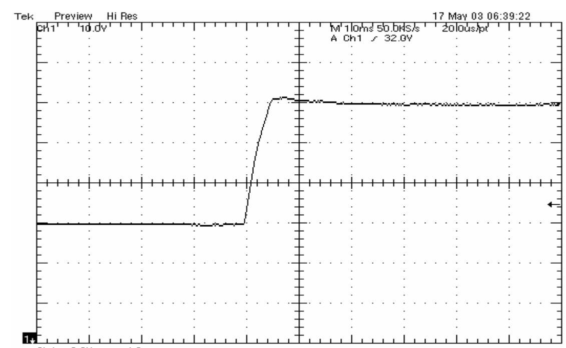

(b) Current mode fuzzy logic controller with ESO

Figure 9. Step change (from 30 to 36V) in output reference voltage for Vin=20V (X axis: 1ms/div, Y axis: 2V/div)

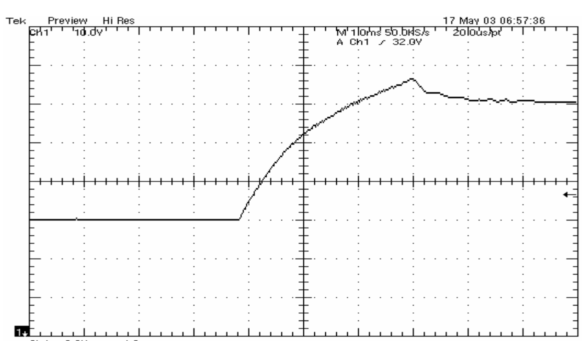

(a) Conventional fuzzy logic controller

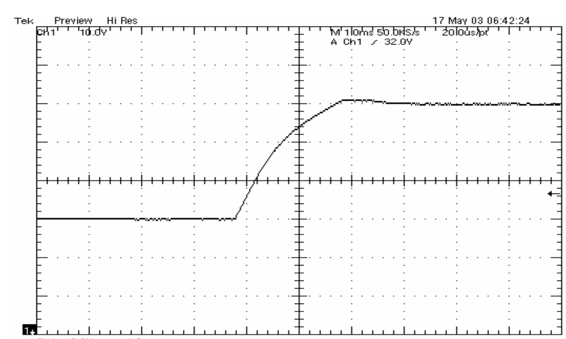

(b) Current mode fuzzy logic controller with ESO

Figure 10. Step change (from 30 to 36V) in output reference voltage for Vin=12V (X axis: 1ms/div, Y axis: 2V/div)